Dissociation and Ionization of H_2^+ by Ultrashort Intense Laser Pulses Probed by Coincidence 3D Momentum Imaging

I. Ben-Itzhak, P. Q. Wang, J. F. Xia, A. M. Sayler, M. A. Smith, K. D. Carnes, and B. D. Esry

J.R. Macdonald Laboratory, Department of Physics, Kansas State University, Manhattan, Kansas 66506, USA

(Received 15 January 2005; published 9 August 2005)

Laser-induced dissociation and ionization of H_2^+ were simultaneously measured using coincidence 3D momentum imaging, allowing direct separation of the two processes, even where the fragment kinetic energy is the same for both processes. The results for 45 and 135 fs 790 nm pulses with an intensity of approximately 2.5×10^{14} W/cm^2 differ from each other much more than one would expect from previous measurements with longer pulses. Ionization was negligible for the longer pulse and was strongly aligned along the laser polarization for the shorter pulse, but showed no structure in its kinetic energy distribution. In addition, the ionization to dissociation ratio was found to be much smaller than theoretically predicted for H_2^+.

DOI: 10.1103/PhysRevLett.95.073002 PACS numbers: 33.80.Wz, 33.80.Eh, 42.50.Hz

Interrogating molecules with intense short-pulse lasers has resulted in a multitude of interesting phenomena due mainly to the comparable strength of the interactions of the electrons with the nuclei and the laser field. Among these phenomena are: tunneling ionization, above threshold dissociation, bond softening and hardening, charge resonance enhanced ionization, and molecular alignment (see the reviews [1,2]). While theorists commonly study these effects in H_2^+ due to its simplicity (e.g., [2–6]), experimentalists, for obvious reasons, study instead the readily available H_2 (e.g., [7–14]). Some of the H_2 studies have tailored the experimental conditions to enable the study of the transient H_2^+ formed early in the laser pulse (see, for example, [10,11]). Much of the physics of H_2^+ in an intense laser, however, is more easily understood starting from H_2^+ directly.

A key difference between the two approaches is that dissociation of H_2^+ produced from H_2 in a laser pulse cannot occur for lower intensities than that needed to first ionize the H_2 target, while H_2^+—especially in excited vibrational states—can dissociate at much lower intensities. Therefore, dissociation of H_2^+ from an ion beam can be expected to differ from that of H_2^+ produced in the same laser pulse from H_2. Moreover, it has been recently shown by Urbain *et al.* [15] that intense laser pulses preferentially populate lower H_2^+ vibrational states than would be expected from the Franck-Condon distribution which is typical for H_2^+ beams produced from H_2 by electron impact ionization in the ion source [16]. Furthermore, the vibrational population produced in the laser pulse is coherent, whereas molecular ions in a beam lose this coherence during their long flight time (typically μs) from the ion source.

In this Letter, we present kinematically complete measurements of laser-induced ionization and dissociation of an H_2^+ target. Pioneering experimental studies of these interactions have been reported [17–19], some of which used 2D momentum imaging of one fragment with sufficient energy resolution to separate individual vibrational states [18,19]. They only partly separated ionization ("Coloumb explosion") from dissociation, however, because the kinetic energy release (KER) distributions overlapped [17,19]. The 3D momentum-imaging technique presented in this Letter, on the other hand, provides complete kinematic information about both heavy molecular fragments. Specifically, using an electric field parallel to the ion beam in the interaction region allows the direct separation of dissociation, $H^+ + H$, and ionization, $H^+ + H^+$, even for identical KER values. This separation is accomplished without compromising the energy resolution, which is comparable to the best previous measurements [18,19].

Using this technique, we have studied the dissociation and ionization of H_2^+ by "short" (45 fs FWHM) and "long" (135 fs FWHM) laser pulses, each with a peak intensity of about 2.5×10^{14} W/cm^2. Surprisingly, the KER and angular distributions for dissociation in these pulses differed dramatically in contrast to the previously reported similarity for pulses longer than 135 fs [18].

In our experiment, a beam of H_2^+ is produced in an electron cyclotron resonance (ECR) ion source (most likely in a Franck-Condon distribution of vibrational states), accelerated to an energy of a few keV, and directed toward a small Faraday cup through a longitudinal spectrometer, where the ion beam was intersected by a 790 nm laser beam, as shown in Fig. 1. The Ti:sapphire laser beam was transported through vacuum to the experimental setup where it was focused by an $f = 200$ mm lens, thus defining an interaction region with a 65 μm waist diameter. Before focusing, the polarization of the laser (typically linear upon arrival) was controlled by a combination of a half- and a quarter-wave plate. Here, we have used light linearly polarized along the x axis, where the laser and ion beams travel along the y and z axes, respectively. The laser

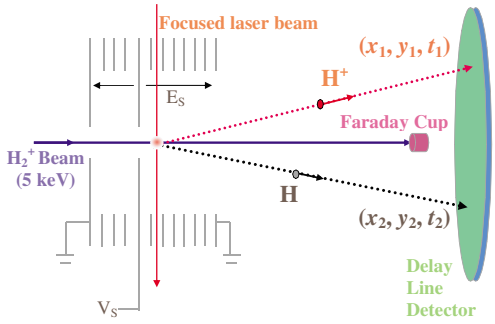

FIG. 1 (color online). Schematic of the experimental setup (see Ref. [20]).

pulse energy was typically around 1 mJ, resulting in peak intensities on the order of 10^{14} W/cm^2 in the focal region with an approximately Gaussian spatial distribution. The laser's repetition rate was 1 to 2 kHz, giving about 20–40 Hz of true coincidences between molecular fragments with a beam current of about 1 nA. A few peak laser intensities were used for both the short (45 fs) and long (135 fs) pulses, keeping the pulse shape the same by placing a neutral density filter or a beam splitter in front of the focusing lens.

The molecular fragments were detected in coincidence by the microchannel plate delay-line detector of a molecular dissociation 3D momentum-imaging system. In addition, coincidence with the laser pulse, detected directly with a photodiode, was required for the true events. The triple coincidence condition was needed to separate the true dissociation events from the much higher rate of (i) dissociation of the H_2^+ beam induced by the residual gas (despite the $\sim 10^{-10}$ Torr vacuum), (ii) residual gas ions produced by the laser pulse, and (iii) particles from slit scattering. The detector signals provide the position and arrival time information for each fragment, and thus their velocity vectors. Using this information, recorded event by event, the true events are distinguished by momentum conservation from random pairs—a correction of special importance for low-rate reaction channels (ionization in our case)—as it discriminates against random coincidences between H^+ fragments from two molecular ions dissociating in a single laser pulse. After all the true events are identified, the velocities are used to evaluate the angular and kinetic energy release distributions.

To distinguish between dissociation and ionization, we introduced a weak uniform electric field pointing along the beam direction in the interaction region (see Fig. 1). The electric field accelerates H^+ fragments so that they hit the detector first, separating them from H fragments by their time of flight (TOF). Dissociation and ionization events are then identified directly by the coincidence TOF condition. Note that the dissociation velocity is much smaller than the beam velocity, broadening the TOF peaks but not changing their time order. To verify that the spectrometer electric field does not distort the measured image significantly, we reproduced the $\cos^2\theta$ (θ is the angle between the molecular axis and the polarization) distribution expected under weak-field conditions. To this end, we used an intensity smaller by about 5 orders of magnitude by not focusing the laser beam.

To help interpret our data, we computed the expected KER spectra by solving the time-dependent Schrödinger equation in the Born-Oppenheimer representation without nuclear rotation [1,2]. A wide range of intensities was considered for both the short and long pulses. For intensities up to about 4×10^{13} W/cm^2, only the $n = 1$ states of H were needed, but for higher intensities, states up to H($n = 3$) were required for convergence. This truncated Born-Oppenheimer representation applies so long as ionization is not significant—up to around 10^{14} W/cm^2. We considered all possible initial vibrational states and combined them according to the Franck-Condon distribution for comparison with experiment.

The angular and KER distributions of the fragments produced by 135 and 45 fs pulses with peak intensities of about $I_0 = 2.5 \times 10^{14}$ W/cm^2 are shown in Figs. 2 and 3, respectively. Even though the intensities are similar, the results are quite different: (i) ionization was detected only for the short pulse; (ii) distinct structure appears at the KER values expected for the unperturbed H_2^+ vibrational states for the long pulse, while the short-pulse KER spectrum is mainly a broad distribution centered around $\sim$0.8 eV; and (iii) the short pulse yields dissociation fragments with a narrow angular distribution and KER values below 0.3 eV where no dissociation is observed for the long pulse.

Since ionization was measurable only for the shorter pulse—and both pulses had similar peak intensities—the data supports the conclusion that the pulse duration has a strong impact on the branching ratio of ionization and dissociation as predicted, for example, by Kulander *et al.* [4]. Additional measurements with higher peak intensities showed a fast increase in ionization, as shown in Figs. 3(c) and 3(d). Explicitly, the ionization fraction increased by about an order of magnitude while the peak intensity less than doubled. This rate of increase goes down with further increases in intensity. In addition, it is evident from Fig. 3 that ionization by a 45 fs pulse peaks more strongly along the laser polarization ($|\cos\theta| = 1$) than does dissociation. Moreover, ionization, integrated over θ, was more than an order of magnitude smaller than dissociation for the intensities presented here. This ratio is much smaller than theoretical predictions, which predict that ionization dominates (e.g., Ref. [6]). In the calculations, however, it was assumed that the molecules were aligned along the field. It is therefore not surprising that the comparison improves if we experimentally select molecules aligned along the field. When restricted to a 12.5° cone, for instance, the ratio of ionization to dissociation increases by about a factor of 5,

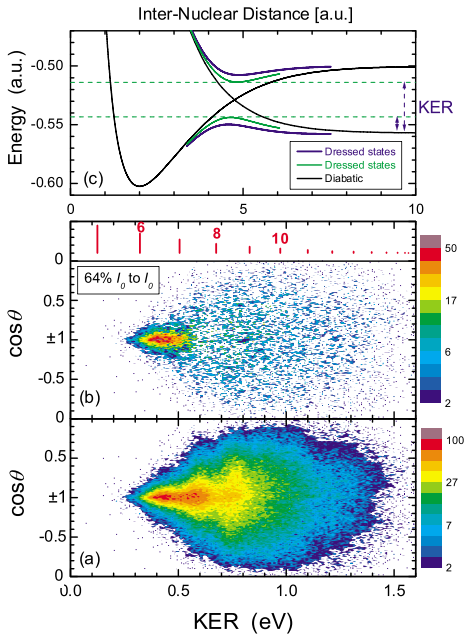

FIG. 2 (color online). (a) Angle vs KER distribution for dissociation in a 135 fs, $I_0 = 2.4 \times 10^{14}$ W/cm^2 laser pulse, (b) including only the intensities between 64% and 100% of I_0. The vertical bars mark the expected KER of the unperturbed vibrational levels (their length represents the population of the state, assuming a Franck-Condon distribution). (c) Field-dressed (Floquet) Born-Oppenheimer curves for intensities relevant to the measurement. The minimum and maximum KER values are associated with the barrier height and well minimum for each I_0.

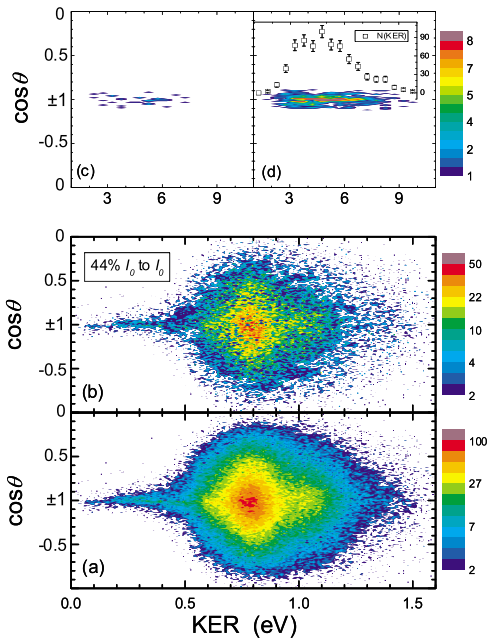

FIG. 3 (color online). Angle vs KER distributions: (a) and (b) are similar to those shown in Fig. 2, but for a 45 fs pulse; (c) and (d) show ionization by a 45 fs pulse of 2.5×10^{14} W/cm^2 and 4.1×10^{14} W/cm^2 peak intensities, respectively.

although dissociation still dominates for $I_0 \lesssim 5 \times 10^{14}$ W/cm^2. The ability to select aligned molecules allows comparisons not otherwise possible, since calculations simultaneously including dissociation and ionization for molecules not aligned with the field are prohibitively expensive computationally.

Our ability to clearly distinguish ionization from dissociation also allows a more direct check of the theoretical prediction of two peaks in the ionization KER distribution [1,3]. These peaks have not yet been observed, but the overlap of above threshold dissociation (ATD) with low-KER ionization made comparison difficult [10,17]. As Fig. 3(d) shows, only one broad high-KER peak is observed. The low-KER peak predicted from theory at about 2.5 eV (as a peak in ionization around $R \approx 11$ a.u.) is absent. Further, there are no signs of the vibrational structure reported recently by Pavičić *et al.* [19].

The second feature of Figs. 2 and 3 mentioned above, is the lack of vibrational state structure for the short pulse. Heuristically, we can understand this difference to be a combination of the experimental resolution and the fact that the 45 fs pulse length is comparable to the vibrational period of the bond-softened states ($\sim$25 fs for $v = 8$). The 135 fs pulse is much longer than these vibrational periods, however, and the KER spectrum displays clear peaks, though they are slightly shifted to lower energies from those expected for $v = 7$–9. Additionally, the angular distribution becomes narrower for lower v, consistent with dissociation by bond softening, i.e., the lowering of the barrier in the field-dressed ground state due to its coupling with the first excited state, Fig. 2(c).

The long pulse data are in good qualitative agreement with the lower intensity measurements of Sändig *et al.* [18]. Where they disagree, though, it is hard to distinguish intensity effects from "volume effects." They used an ion beam as narrow as the laser-beam waist, while our ion beam was much wider than the laser beam, resulting in larger contributions from low intensities in the present results. These differences prevent quantitative comparison between the two measurements.

The volume effect can be dealt with theoretically by averaging the results for several intensities over the focal volume for direct comparison with experiment (e.g., [21]). It can also be dealt with by purely experimental means by subtracting two measurements conducted under the same conditions but with different peak intensities to construct the intensity difference spectrum (IDS) [22]. This method takes advantage of the spatial intensity distribution of a Gaussian beam and the approximately constant longitudinal laser intensity when a thin target is used, i.e., thinner than the Rayleigh length. We use the experimental approach here, and show examples in Figs. 2(b) and 3(b) where the low-intensity contributions have been subtracted.

Using the IDS to focus on just the high laser intensities enhances the differences between the long and short pulses. The former leads to dissociation that is strongly aligned along the laser polarization with a KER of about 0.3 to 0.5 eV [Fig. 2(b)]. In contrast, the latter results mainly in a broad KER distribution extending from 0.5 to 1.2 eV that is not as strongly aligned with the laser field [Fig. 3(b)]. Also for the short pulse, there is a small contribution of strongly aligned dissociating molecules spanning the KER range from almost zero up to about 0.4 eV. In contrast to this strong dependence on pulse length, Sändig *et al.* [18] observed almost no dependence on pulse duration for longer pulses (135 fs to 600 fs) but a strong dependence on intensity. They observed, for example, identical angular distributions for 135 and 405 fs pulses of the same intensity.

The very low-KER feature in the present 45 fs pulse data vanishes for higher intensity IDS than shown in Fig. 3(b), but the broad dominant feature around 0.8 eV persists. We thus conclude that this broad peak is due to ATD. Our solutions of the time-dependent Schrödinger equation support this conclusion and indicate that it is due to ATD with net two-photon absorption.

These solutions also show strong, intensity-dependent shifts of the peaks in the KER spectra from each initial vibrational state, with some peaks splitting at the highest intensities. Identifying a given peak with its initial state or by its physical mechanism based solely on its field-free KER is thus difficult at best and misleading at worst.

Finally, the energy and angle dependence of the dissociation spectra in Figs. 2(a) and 3(a) can be understood from the Floquet potentials in Fig. 2(c). The electric field along the molecular axis is associated with the angle θ through $E_{\text{eff}} = E_0 \cos\theta$ (where $E_0 \propto \sqrt{I_0}$), assuming molecular rotation during the laser pulse is negligible. Therefore, dissociation at large θ is associated with a smaller energy gap between the dressed potential energy curves [see, Fig. 2(c)] due to the weaker field along the molecular axis. Bond softening is just dissociation in this energy gap—the barrier height and well minimum thus roughly determine the minimum and maximum KER, respectively. As a result, the range of possible KERs decreases with increasing θ as the energy gap closes, converging to zero at the KER expected for the diabatic curve crossing at $\cos\theta = 0$. From the figure, it is clear that the high-KER edge at a given $\cos\theta$ is not as sharp as the low-KER edge. Since some of the H_2^+ population can become temporarily trapped in the upper well (bond hardening) during the pulse, dissociation at these energies is not as efficient. In contrast, at the low-KER edge, dissociation sets in relatively quickly since it is controlled by tunneling through the potential barrier.

To summarize, we have presented an experimental method for the study of molecular ion interactions with ultrashort intense laser pulses. This method is based on coincidence molecular dissociation 3D momentum imaging and uses a weak longitudinal electrostatic field to directly distinguish ionization from dissociation. Further, difference spectra can be constructed that reduce the intensity averaging effect. We found ionization to be much smaller relative to dissociation than predicted theoretically. Moreover, we found no evidence for structure in the ionization KER distribution, neither the two peaks predicted for enhanced ionization nor the vibrational structure recently reported. Dissociation and ionization are much more sensitive to the reduction of the pulse duration from 135 to 45 fs than from 405 to 130 fs [18]. This is attributed to the fact that the 45 fs pulse duration is approaching the vibrational time scale.

The authors wish to thank Dr. B. Shan and Professor Z. Chang for providing the intense laser beams for this experiment, and Dr. C. Fehrenbach for the ECR beam. This work was supported by the Chemical Sciences, Geosciences, and Biosciences Division, Office of Basic Energy Sciences, Office of Science, U.S. Department of Energy.

[1] J. H. Posthumus, Rep. Prog. Phys. **67**, 623 (2004).
[2] A. Giusti-Suzor, F. H. Mies, L. F. DiMauro, E. Charron, and B. Yang, J. Phys. B **28**, 309 (1995).
[3] T. Zou and A. D. Bandrauk, Phys. Rev. A **52**, R2511 (1995).
[4] K. C. Kulander, F. H. Mies, and K. J. Schafer, Phys. Rev. A **53**, 2562 (1996).
[5] S. Chelkowski, P. B. Corkum, and A. D. Bandrauk, Phys. Rev. Lett. **82**, 3416 (1999).
[6] B. Feuerstein and U. Thumm, Phys. Rev. A **67**, 043405 (2003).
[7] P. H. Bucksbaum, A. Zavriyev, H. G. Muller, and D. W. Schumacher, Phys. Rev. Lett. **64**, 1883 (1990).
[8] A. Zavriyev *et al.*, Phys. Rev. A **42**, 5500 (1990).
[9] J. Ludwig, H. Rottke, and W. Sandner, Phys. Rev. A **56**, 2168 (1997).
[10] G. N. Gibson, M. Li, C. Guo, and J. Neira, Phys. Rev. Lett. **79**, 2022 (1997).
[11] J. H. Posthumus *et al.*, J. Phys. B **33**, L563 (2000).
[12] F. Rosca-Pruna, and M. J. J. Vrakking, Phys. Rev. Lett. **87**, 153902 (2001).
[13] A. Staudte *et al.*, Phys. Rev. A **65**, 020703(R) (2002).
[14] A. S. Alnaser *et al.*, Phys. Rev. Lett. **93**, 183202 (2004).
[15] X. Urbain *et al.*, Phys. Rev. Lett. **92**, 163004 (2004).
[16] F. von Busch and G. H. Dunn, Phys. Rev. A **5**, 1726 (1972).
[17] I. D. Williams *et al.*, J. Phys. B **33**, 2743 (2000).
[18] K. Sändig, H. Figger, and T. W. Hänsch, Phys. Rev. Lett. **85**, 4876 (2000).
[19] D. Pavičić, A. Kiess, T. W. Hänsch, and H. Figger, Eur. Phys. J. D **26**, 39 (2003).
[20] I. Ben-Itzhak *et al.*, Nucl. Instrum. Methods Phys. Res., Sect. B **233**, 56 (2005).
[21] V. N. Serov *et al.*, Phys. Rev. A **68**, 053401 (2003).
[22] P. Q. Wang *et al.*, Opt. Lett. **30**, 664 (2005).